

Hybrid Alginate–Brushite Beads Easily Catalyze the Knoevenagel Condensation On-Water

Yousra El Jemli, Khadija Khallouk, Salaheddine Lanaya, Mathieu Brulé, Abdellatif Barakat,*
Karima Abdelouahdi, and Abderrahim Solhy



Cite This: *ACS Omega* 2022, 7, 27831–27838



Read Online

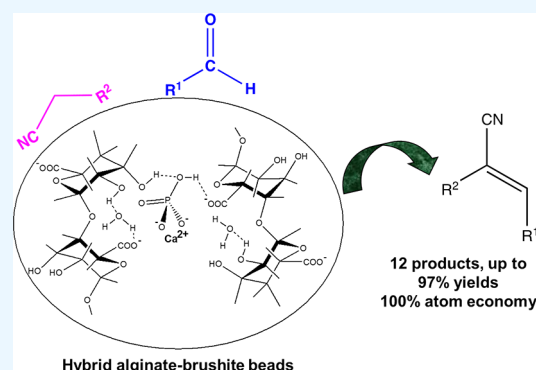
ACCESS |

Metrics & More

Article Recommendations

Supporting Information

ABSTRACT: An innovative hybrid organic–inorganic material composed of alginate–brushite xerogel beads was successfully applied for the catalysis of the Knoevenagel condensation. The catalyst was derived from phosphated alginate xerogel microspheres formed from the ionotropic gelling effect of phosphated alginate. To this end, alginate was phosphated by the addition of diammonium hydrogen phosphate in a 1% w/w alginate gel. The phosphated alginate was subsequently precipitated by chelation of Ca^{2+} cations, generating a phosphated alginate hydrogel microsphere, which was washed and dried, forming hybrid organic–inorganic xerogel beads as a crystalline phosphate-rich mineral fraction covered by alginate. X-ray diffraction analysis revealed that the crystalline inorganic matrix of the material was composed predominantly of brushite. SEM analysis revealed plate-like, ribbon-like, or needle-like morphologies in the hybrid alginate–brushite beads. The hybrid material was tested as a catalyst for Knoevenagel condensation, which was performed “on-water” under mild conditions with aromatic aldehydes and activated methylene compounds, giving high yields (up to 97%). The reaction rate and product yield increased together with the reaction temperature for all reagents. The recyclable solid catalyst was effective for three runs, revealing the potential of the innovative hybrid catalyst as an eco-friendly heterogeneous catalyst.



1. INTRODUCTION

A hybrid material is a system in which organic and inorganic species both coexist.^{1,2} The hybrid nature of these materials confers them intermediate properties between inorganic and organic, along with new behaviors.^{1,3} Their structures essentially involve either weak or strong electrostatic interactions resulting from the incorporation of one of the two phases in the other, or onto a graft polymer, with incorporation of the organic and inorganic phases. Depending on the nature of the interface, these materials have been divided in two distinct classes (class I or II). In class I materials, the organic and inorganic fractions are connected by weak bonds. In class II materials, these fractions are linked together by strong chemical bonds, being either covalent or ionic-covalent bonds.^{4,5} Hybrid materials are used in several cutting-edge technological fields,^{6–12} with important applications in the catalysis.^{13–17} For example, a hairy particle formed from a zeolite-like organic–inorganic hybrid material with a high organic content was synthesized by one-step dry-gel conversion (DGC) assembly without any organic template.¹⁸ This hybrid material was sulfonated and subsequently used as a solid-acid catalyst for the condensation of cyclohexanone and glycol, and coordinated by Co^{2+} ions for the selective catalysis of alkene epoxidation in air. Li *et al.*¹⁹ found that the reduction of 4-nitrophenol by NaBH_4 can be achieved by Ag–Au

bimetallic nanocomposites, which were stabilized with organic–inorganic hybrid microgels. The authors reported the synthesis of Ag@poly (nisopropylacrylamide-co-3-methacryloxypropyltrimethoxysilane) hybrid microgels by seed-emulsion polymerization using Ag nanoparticles (NPs) as the core and NIPAM/MAPTMS as monomers. Furthermore, bimetallic hybrid microgels of Ag–Au@P(NIPAM-co-MAPTMS) were prepared by the addition of HAuCl_4 , resulting in a partial substitution of Ag. The catalytic performance of this hybrid material was related to the presence of the thermosensitive PNIPAM chains, along with the highly porous structure constructed by rigid MAPTMS segments intersected between NIPAM chains. Xu *et al.*²⁰ described a highly active and reusable catalyst for deacetalization–Knoevenagel condensation as a one-pot tandem reaction using multilayered zeolites with organic-structure-directing agent molecules occluded within micropores. The presence of both base sites and acid sites indicated that these hybrid

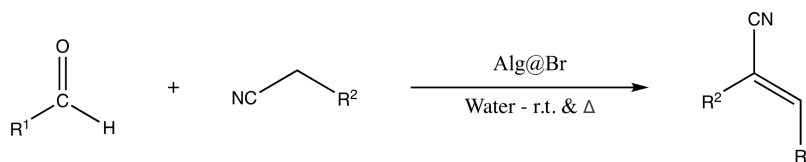
Received: December 30, 2021

Accepted: March 14, 2022

Published: August 5, 2022



Scheme 1. Knoevenagel Condensation "On-Water"



catalysts were bifunctional. The organic–inorganic hybrid zeolite matrix was impregnated by palladium nanoparticles, producing a catalyst that was extremely active for one-pot synthesis of benzylidene malononitrile from benzyl alcohol *via* alcohol oxidation followed by Knoevenagel condensation with malononitrile.

There is a recent interest in the application of biopolymers for the production of hybrid catalyst materials. In particular, chitosan has been used as organic biopolymer matrices for the production of hybrid catalyst materials.^{21,22} Furthermore, alginate beads have also been integrated as the organic component of hybrid catalysts; in particular, Ag and Au nanoparticles have been stabilized with calcium alginate, and the resulting hybrid material was applied for the catalysis of 4-nitrophenol reduction.²³ On the other hand, the Knoevenagel condensation is one of the most important reactions in the field of organic synthesis^{24–26} given the importance of the α,β -unsaturated carbonyl compounds produced by this reaction.^{27–29} This chemical transformation can be performed under homogeneous^{30–33} or heterogeneous^{34–38} reaction conditions.

The use of water as a solvent in organic synthesis has become a tangible reality.³⁹ Several research works were carried out in this area.⁴⁰ Water, a very abundant solvent that is cheap, nontoxic, and nonflammable, can appear as the ideal "alternative" solvent for performing reactions of organic synthesis.⁴¹ It has been reported that the Diels–Alder reaction was considerably accelerated in water, in comparison with organic solvents, while being as well more selective in favor of the endo isomer.⁴² The origin of the acceleration, as well as the increased selectivity, was attributed to hydrophobic interactions.^{43,44} Many studies have emphasized the role of hydrophobic effects in water.⁴⁵ Sharpless *et al.*⁴⁶ developed the concept of "on-water" chemistry after conducting several cycloaddition experiments in different solvents. The hydrophobic effect plays an important role, but other effects involving the presence of hydrogen bonds may also accelerate reactions between insoluble molecules.⁴⁷ Thus, many reactions can be carried out advantageously "on-water".⁴⁸ Alternately, Hayashi⁴⁹ proposed to qualify these reactions as "in-water". Indeed, various hydrophobic^{43,44} or hydrophilic substrates^{50–54} have been tested to validate these two concepts. Hence, "on-water" or "in-water" reactions have led to important industrial developments.⁵⁵ In particular, the importance of reactions in an aqueous medium is illustrated by the industrialization of several processes based on the use of chelated metals by water-soluble ligands bearing ionic groups (e.g., trisulfonated triphenylphosphine).^{56–58}

In continuation of our previous works,^{59–61} in the present study, we propose the development of a new catalytic system in the form of a microreactor with high-performance catalytic ability under mild conditions for the synthesis of the α,β -unsaturated carbonyl compounds. For this purpose, hybrid xerogel beads (alginate@brushite: Alg@Br) were synthesized *via* phosphated alginate gelation, and their structural, thermal,

and morphological characterizations were studied. Subsequently, the hybrid xerogel beads were used as a catalytic microreactor for achieving Knoevenagel condensation "on-water" (Scheme 1). Furthermore, the stability of the catalyst was examined in several successive catalytic runs.

2. EXPERIMENTAL SECTION

2.1. Material Characterization. All reagents were purchased from Sigma-Aldrich and had very high purity levels (<97%). Fourier transform infrared spectroscopy (FTIR) analysis was performed in the 400–4000 cm^{-1} range on a Bruker Vector 22 spectrometer. The background spectrum was collected on a pure KBr pellet (sample/KBr ratio: 0.3%). A scan number of 20 is considered optimal to obtain a good quality spectrum. X-ray diffraction patterns were obtained at room temperature on a Bruker AXS D-8 diffractometer using Cu $K\alpha$ radiation in Bragg–Brentano geometry (θ – 2θ). Scanning electron microscopy (SEM) pictures were recorded on an FEI Quanta 200 microscope after carbon metallization. Gas adsorption data were collected using a Micromeritics 3Flex Surface characterization analyzer using N_2 . Prior to N_2 sorption, all samples were degassed at 150 $^\circ\text{C}$ overnight. Specific surface areas were determined from the nitrogen adsorption/desorption isotherms (at -196 $^\circ\text{C}$) using the BET (Brunauer–Emmett–Teller) method. ^1H NMR spectra were recorded on a 300 MHz spectrometer by using a Bruker ARX 300 spectrometer at ambient temperature and in CDCl_3 as solvent.

2.2. Synthesis of Hybrid Alginate–Brushite Beads.

The hydrogel material was generated *via* the complexation of phosphate-alginate by Ca^{2+} cations (Figure S1). To this end, an aqueous solution of phosphorus precursor was prepared by dissolving $(\text{NH}_4)_2\text{HPO}_4$ (0.3 M) into 100 mL of distilled water, and then, sodium alginate was added to a diammonium hydrogen phosphate solution with a concentration of 1% (w/w), resulting in the phosphatation of the alginate. The mixture was stirred for 1 h at room temperature. This gel was added dropwise using a syringe with a 0.8 mm diameter needle at room temperature to the stirred $\text{Ca}(\text{NO}_3)_2 \cdot 4\text{H}_2\text{O}$ solution (0.25 M). Bead structures started to form, and the mixture was immediately abandoned overnight to ensure the effective diffusion of calcium ions and thereafter the homogeneity of the system, along with the growth of the hybrid material. The beads were then filtered with a 100-mesh screen and washed three times with distilled water to remove excess Ca^{2+} ions and impurities from the surfaces. Finally, the beads were dried at room temperature for 24 h, yielding hybrid alginate–brushite xerogel beads (Alg@Br) as evidenced by the subsequent chemical characterization. For comparison purposes, following a similar approach, xerogel beads containing calcium alginate only (Alg@Ca), in the absence of the brushite component, were produced by dropwise addition of 1% sodium alginate solution into 0.25 M Ca^{2+} solution and subsequent drying of hydrogel beads at room temperature.

2.3. General Procedure for Knoevenagel Condensation On-Water. The catalyst (25 mg) was added to a stirred mixture of arylaldehyde (1.5 mmol), active methylene compounds (1.5 mmol), and water as solvent (1 to 3 mL). The reaction mixture was carried out at various temperatures. The reaction was monitored by thin layer chromatography. Upon completion of the reaction, EtOAc (3×10 mL) was added, the catalyst was filtered off, and the solution was concentrated to afford a residue, which was purified by distillation under vacuum followed with recrystallization. The products were identified by ^1H NMR. The structures of the obtained products were assigned on the basis of their spectral data in comparison with those reported in the literature.^{26–30} The recovered catalyst was washed twice with dichloromethane and water and dried at 80°C before being reused in subsequent runs to demonstrate its prolonged activity.

3. RESULTS AND DISCUSSION

The ionotropic gelling of alginate, a natural block polysaccharide with carboxylic functions, implies the chelation of calcium cations by the carboxylate groups of two chains of polysaccharides, resulting in the formation of electrostatic bridges between chains in the hydrogel network. Since alginate was phosphated by the addition of diammonium hydrogen phosphate, it is quite likely that HPO_4^{2-} ligands may have attached to the alginate fibrils *via* hydrogen bonds (Figure S2), generating a stable phosphated gel, capable of further chelating calcium, and subsequently forming brushite *in situ* after drying of the hydrogel. As-obtained hybrid alginate–brushite beads (Alg@Br) after conventional drying of hydrogel beads were analyzed by FTIR (Figure 1). The absorptions observed at

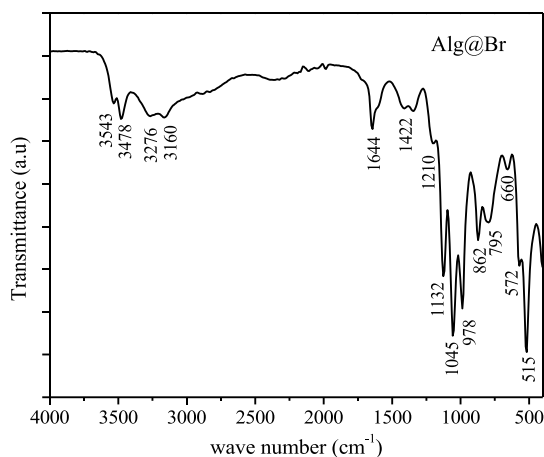


Figure 1. FT-IR spectrum of xerogel-beads (Alg@Br).

1422 and 1644 cm^{-1} are related to the symmetric and asymmetric stretching modes of the COO^- bands from the carboxylate groups.^{62,63} The spectrum of Alg@Br is characterized by the O–H stretching modes of the water molecules in the brushite crystal lattice, with two peak doublets, respectively, at 3543 and 3478 cm^{-1} and at 3276 and 3160 cm^{-1} .⁶² The main IR bands characterizing the PO_4 group can be detected at 1132 , 1045 , 978 , and 795 cm^{-1} due to PO stretching modes of the PO_4 .⁶⁴ Weaker sharp bands at 1210 and 862 cm^{-1} are due, respectively, to the P–O(H) stretching mode and in-plane P–O–H bending mode.⁶⁵ Bands at frequencies 515 , 572 , and 660 cm^{-1} are assigned mainly to PO deformation modes of the tetrahedral PO_4 group.⁶⁶

Figure 2 shows the X-ray powder diffractogram of hybrid alginate–brushite beads. This analysis revealed the presence of

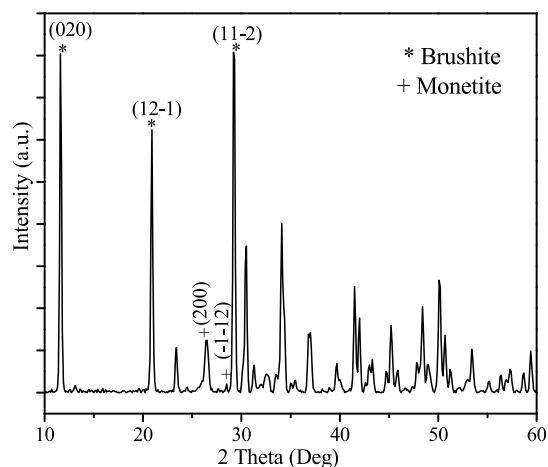


Figure 2. XRD patterns of hybrid alginate–brushite beads Alg@Br.

the brushite phase (dicalcium phosphate dihydrate: $\text{CaHPO}_4 \cdot 2\text{H}_2\text{O}$), which has a monoclinic crystal structure (JCPDS 4-013-3344). Brushite crystallized in the monoclinic system (space group Ia) with the crystallographic parameters $a = 6.239\text{ \AA}$, $b = 15.180\text{ \AA}$, $c = 5.812\text{ \AA}$, $\alpha = \gamma = 90^\circ$, and $\beta = 116^\circ 42'$. The intensity of the diffraction peaks indicates that Alg@Br is well crystallized. Furthermore, the presence of a minor fraction with a monetite phase (dicalcium phosphate: CaHPO_4) should be noted. Monetite crystallized in the triclinic system (space group $P-1$) with the crystallographic parameters $a = 6.91\text{ \AA}$, $b = 6.998\text{ \AA}$, $c = 6.627\text{ \AA}$, $\alpha = 96.34^\circ$, $\beta = 91.67^\circ$, and $\gamma = 76.18^\circ$ (JCPDS 4-009-4184).

The conventional drying has brought about a volume shrinkage of the hydrogel as shown in the digital photo (Figure 3a). The SEM of hybrid alginate–brushite beads at low magnification (Figure 3b) revealed that beads have a lentil form with a micrometric size. The morphologies of the cross section of a bead are plate-like, ribbon-like, or needle-like structures (Figure 3c,d). Indeed, brushite, forming the inorganic component of hybrid xerogels, is generally described as sheets of uniform needle- and plate-like crystals.⁶⁷

Adsorption and desorption isotherms were measured with nitrogen gas. The analysis did not reveal any porosity in the hybrid alginate–brushite beads. This can be explained either by the nonporosity of this material or by the existence of macropores greater than 50 nm . However, this technique based on the BET model (Brunauer–Emmett–Teller) is not reliable to analyze materials containing macropores with a pore size greater than 50 nm (corresponding to the relative pressures $P/P_0 > 0.98$, following the Kelvin equation). The appropriate technique for the macroporous materials ($>50\text{ nm}$) would be mercury porosimetry.

The thermogravimetry analysis (TGA) of the hybrid alginate–brushite material, already performed in previous works,⁵⁹ has revealed that its main fraction may be composed of the organic alginate phase, with the mineral fraction (brushite and monetite) accounting for only 20–25% w/w of the hybrid material.

Knoevenagel condensation was carried out between substituted aldehydes and activated methylene compounds and catalyzed by Alg@Br “on-water” at different temperatures:

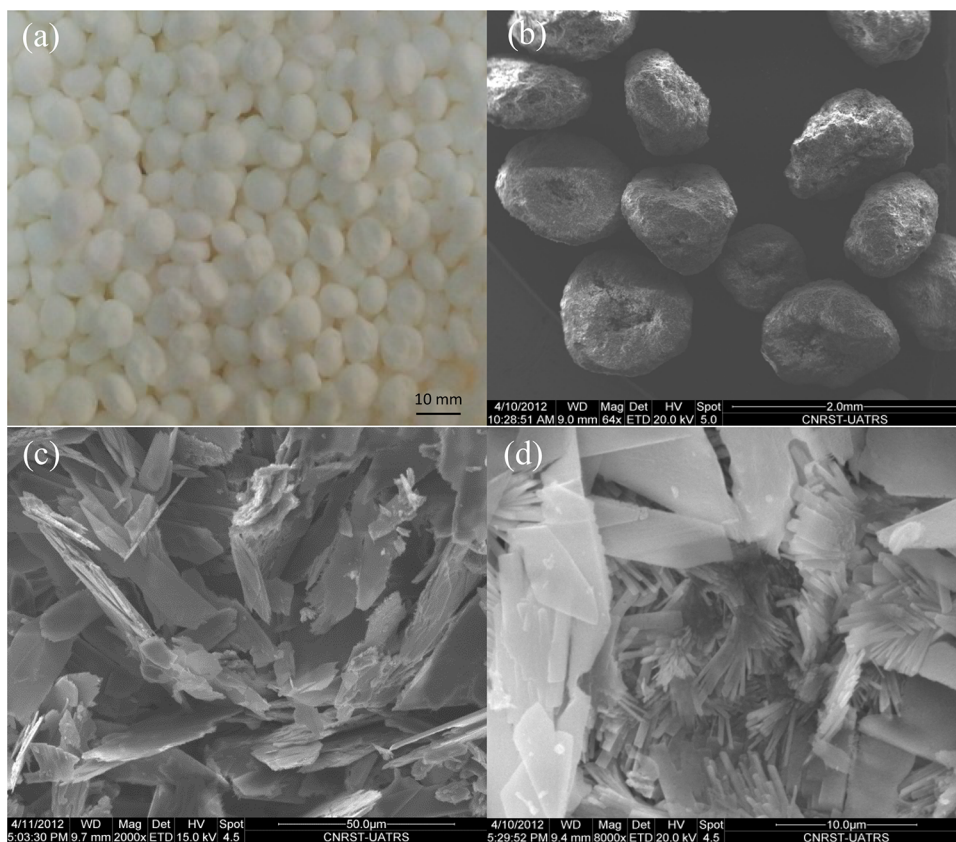


Figure 3. Digital image (a) and SEM observation under various magnification levels (b, c, d) of xerogel beads synthesized *via* gelation of phosphated alginate.

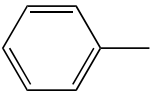
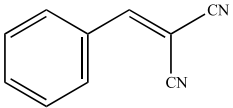
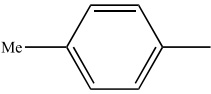
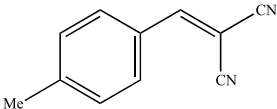
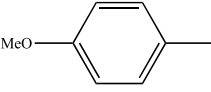
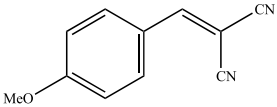
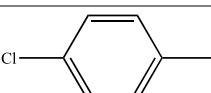
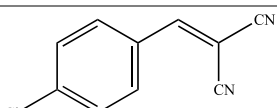
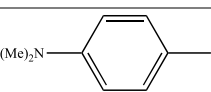
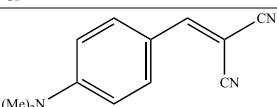
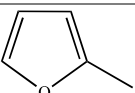
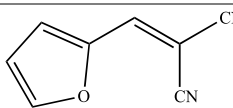
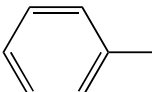
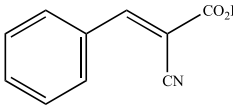
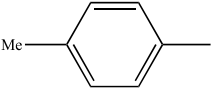
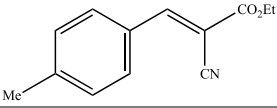
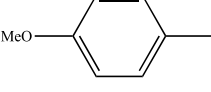
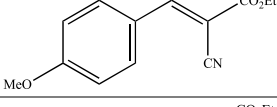
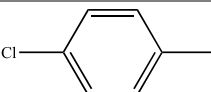
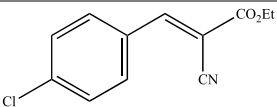
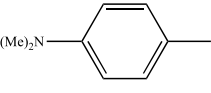
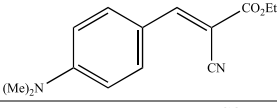
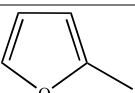
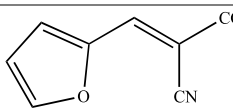
room temperature and 40 and 100 °C. The synthesis of 2-(*p*-tolylmethylene) malononitrile was selected as a model reaction so as to optimize the reaction conditions for high yields of α,β -unsaturated carbonyl compounds by studying kinetic factors, which may influence the reaction kinetics of this chemical transformation: temperature, catalyst loading, and nature and volume of the solvent. As a consequence, we developed a new approach for the synthesis of α,β -unsaturated ketones *via* Knoevenagel reaction under mild conditions.

The synthesis of 2-(*p*-tolylmethylene) malononitrile was conducted at a time interval of 15 to 90 min, at room temperature, in 3 mL of water using 25 mg of Alg@Br. The results obtained show increased alkene yields depending on the extension of the reaction time, reaching up to 89% after 90 min. The synthesis of 2-(*p*-tolylmethylene) malononitrile was tested in different solvents such as water, methanol, ethanol, 1-butanol, DMF, and diethylene glycol. Excellent yields ($\sim 90\%$) were obtained in all solvents (3 mL) for 90 min at room temperature. In particular, the reaction performed well in protic and polar solvents. Considering the importance of developing catalysis in environmentally friendly solvents, water was selected as a solvent for further experiments. Under the same conditions (3 mL of water at room temperature), the synthesis of 2-(*p*-tolylmethylene) malononitrile was carried out by varying the catalyst load. The following masses of catalyst were tested: 10, 25, 35, and 50 mg. The conversion yields obtained were, respectively, 48, 89, 92, and 96%. Hence, further increasing the catalyst load beyond 25 mg does not have a significant effect on the catalyst performance. This prompted us to apply a catalyst load of 25 mg in the further experiments. The synthesis of 2-(*p*-tolylmethylene) malononi-

trile was performed at room temperature for 90 min and in the presence of 25 mg of hybrid beads while varying the volume of water. According to the results obtained, nearly quantitative yields were obtained at a volume of water between 1 and 3 mL, with the yields dropping progressively at water volumes above 3 mL. Applying 5, 7, 10, and 20 mL of water in the reaction resulted in decreasing conversion yields of 75, 66, 60, and 25%, respectively. Hence, large water volumes may create a barrier between reagents and catalyst in view of their dispersion, causing a low probability to react. Comparatively, under the same conditions, the yields obtained in 2-(*p*-tolylmethylene) malononitrile synthesis by substituting the Alg@Br hybrid catalyst with brushite-free Alg@Ca xerogels were very low, amounting to only 15% throughout the 90 min reaction time at room temperature. Hence, it appears that the hybrid catalyst Alg@Br may display a higher catalytic activity compared with Alg@Ca.

One of the most critical factors affecting the kinetics of the reaction is the temperature of the reaction medium: the higher the temperature of the reaction medium is, the shorter is the duration of the transformation, and consequently, the more the reaction may be accelerated. The increase in temperature may also trigger blocked chemical transformations provided that these reactions are favorable from a thermodynamic point of view. The opposite effect is also applied for certain transformations. The kinetics of 2-(*p*-tolylmethylene) malononitrile synthesis was slow when performed at room temperature using the hybrid Alg@Br catalyst. Thus, the reaction was tested under similar conditions at higher temperatures of 40 and 100 °C. Increasing the reaction temperature resulted in a higher rate of 2-(*p*-tolylmethylene) malononitrile synthesis.

Table 1. Synthesis of Alkenes *via* Knoevenagel Reaction by Using Alg@Br as Catalyst at Various Temperatures

Entry	R ¹	R ²	Product	Yields (time)		
				[(%)(min)] ^a	[(%)(min)] ^a	[(%)(min)] ^a
				r.t.	40 °C	100 °C
1		—CN		85 (90)	81 (30)	77 (5) 94 (10)
2		—CN		89 (90) 15 (90) ^b	91 (30)	97 (10)
3		—CN		60 (180)	35 (30) 68 (90)	87 (10)
4		—CN		63 (180)	32 (30) 70 (90)	95 (10)
5		—CN		83 (180)	40 (30) 91 (90)	87 (10)
6		—CN		92 (90)	98 (30)	95 (10)
7		—CO ₂ Et		45 (90) 63 (120)	56 (30) 95 (60)	83 (10)
8		—CO ₂ Et		55 (90)	54 (30) 97 (60)	75 (10)
9		—CO ₂ Et		25 (180)	21 (30) 75 (90)	79 (10)
10		—CO ₂ Et		30 (180)	18 (30) 72 (90)	77 (10)
11		—CO ₂ Et		20 (180)	24 (30) 70 (90)	85 (10)
12		—CO ₂ Et		53 (90)	86 (30)	97 (10)

^aYields of pure products isolated by distillation under vacuum, recrystallized in CCl₄, and identified by ¹H NMR. ^bReaction catalyzed by xerogels obtained from alginate gelation with Ca²⁺ cations.

Indeed, isolated alkene yields amounted to 89% for the 90 min reaction time at room temperature compared with 91% for 30 min at 40 °C and 97% for 10 min at 100 °C. Indeed, as the reaction temperature was increased from room temperature up to 100 °C, the transformation time was reduced. Consequently, with increased temperatures, higher product yields could be achieved even at shorter reaction times. The synthesis

of α,β -unsaturated ketones in the presence of hybrid alginate–brushite beads as catalysts was further performed using a broad range of reagents while adopting the optimized reaction conditions, which were determined previously. This experiment explored the versatility and limitation of various reagents, including other aldehydes, and ethyl 2-cyanopropanoate as

activated methylene. The obtained results are shown in Table 1.

Knoevenagel condensation is sensitive to the nature of the substituent groups on the aromatic aldehyde (electron donating or withdrawing groups). The reactivity of each aldehyde together with malononitrile is related to its structure and its electronic properties. Each substituent group may exert diverse effects on the distribution of the electronic density of the aromatic aldehyde (donor (+M) and donor (+I)). In all cases, ethyl-cyanoacetate provided slightly lower yields and reaction rates than malononitrile, especially when aldehydes have substituents with an electron group releasing effect (+M). The kinetics of the reactions was accelerated significantly with higher temperature, resulting in increased yields, with a slight difference in effects depending on the reagent's nature. For the synthesis of 2-(furan-2-ylmethylene) malononitrile, the yields obtained were around ~95% at 100 °C.

Generally, solid catalysts are required to display three main characteristics: high activity, high selectivity, and high stability, allowing for efficient separation, recovery, and recycling. In this context, Alg@Br could be recovered, washed, and dried up at 80 °C before being tested for the 2-(*p*-tolylmethylene) malononitrile synthesis at 100 °C in the same conditions. After a three-cycle run, the catalyst retained its geometric shape and its stability (Figure S3), but a slight decrease in yields was observed (97, 90, and 89%), which might be due to the accumulation of organic substrates covering the active sites of the catalyst.

The mechanism of action of the hybrid catalyst might be related to the presence of Lewis acid catalytic sites, possibly originating from complexed Ca²⁺ cations, together with Lewis base catalytic sites (COO⁻), which could not bind due to steric hindrance within the hybrid alginate–brushite beads, possibly in relation to the inflexible crystalline structure of the mineral fraction of the catalyst (brushite). This phenomenon is similar to a frustrated Lewis-pair catalyst.⁶⁸ This property might facilitate the formation of carbanion, which may be the rate-limiting step, while also allowing the simultaneous activation of the carbonyl group of the aldehyde for the formation of the α,β -unsaturated carbonyl compound.

4. CONCLUSIONS

In conclusion, exploiting the alginate's ability to gel, a stable phosphated gel was obtained by the addition of a phosphate source into the alginate gel, which was subsequently gelled by the complexation of Ca²⁺ cations. Drying of the hydrogel beads generated a hybrid organic–inorganic material, whose inorganic matrix was composed of brushite. Those hybrid alginate–brushite beads were used to develop an innovative approach for the catalysis of the Knoevenagel condensation. Aldehydes underwent a reaction with activated methylenes in the presence of the hybrid catalyst. Several parameters were optimized for the synthesis of 2-(*p*-tolylmethylene) malononitrile and subsequently generalized for the synthesis of a variety of activated alkenes. Increased reaction temperatures, up to 100 °C, significantly improved reaction rates and yields. A variety of α,β -unsaturated carbonyl compounds were synthesized by using this hybrid catalyst "on-water". We hypothesize that hybrid alginate–brushite beads may contain Lewis acid catalytic sites (Ca²⁺) and Lewis base catalytic sites (uncoordinated COO⁻), which may not bind each other due to geometric constraints occurring within the hybrid alginate–brushite beads. Hence, the hybrid catalyst may reflect the

behavior of a frustrated Lewis pair catalyst. The current approach offers many obvious advantages compared with other catalytic systems reported in the literature, such as the cost-efficient mild reaction process, affordable catalyst components and simple catalyst production, use of water as affordable solvent, successful recovery and reuse of the catalyst in three cycle runs, and environment-friendly nature of the catalytic process.

■ ASSOCIATED CONTENT

Supporting Information

The Supporting Information is available free of charge at <https://pubs.acs.org/doi/10.1021/acsomega.1c07247>.

Scheme of the adopted process of the synthesis of the hydrogel beads; Ca²⁺ cation chelation by the formation of multiple coordination bonds between phosphated alginate gel and those cations; photo of hybrid-xerogel beads obtained after three successive uses at 100 °C; and ¹H NMR spectral data of synthesized α,β -unsaturated ketones (PDF)

■ AUTHOR INFORMATION

Corresponding Author

Abdellatif Barakat – UMR IATE, University of Montpellier, INRAE, Agro Institute Montpellier, Montpellier 34060, France; Mohamed VI Polytechnic University, Ben Guerir 43150, Morocco; orcid.org/0000-0003-4196-4351; Email: Abdellatif.barakat@inrae.fr

Authors

Yousra El Jemli – IMED-Lab, FST, Cadi Ayyad University, Marrakech 40000, Morocco

Khadija Khallouk – UMR IATE, University of Montpellier, INRAE, Agro Institute Montpellier, Montpellier 34060, France; LMPCE, EST, Université Sidi Mohammed Ben Abdellah, Fes 30000, Morocco; orcid.org/0000-0002-4919-8594

Salaheddine Lanaya – UMR IATE, University of Montpellier, INRAE, Agro Institute Montpellier, Montpellier 34060, France; Organic Chemistry and Analytical Laboratory, FST, University of Sultane Moulay Slimane, Béni-Mellal 23000, Morocco

Mathieu Brulé – UMR IATE, University of Montpellier, INRAE, Agro Institute Montpellier, Montpellier 34060, France

Karima Abdelouahdi – IMED-Lab, FST, Cadi Ayyad University, Marrakech 40000, Morocco

Abderrahim Solhy – UMR IATE, University of Montpellier, INRAE, Agro Institute Montpellier, Montpellier 34060, France

Complete contact information is available at: <https://pubs.acs.org/10.1021/acsomega.1c07247>

Author Contributions

All authors contributed equally to this work and also to the writing of the manuscript. All authors have given approval to the final version of the manuscript.

Notes

The authors declare no competing financial interest.

REFERENCES

- (1) Livage, J.; Henry, M.; Sanchez, C. Sol-gel chemistry of transition metal oxides. *Prog. Solid State Chem.* **1988**, *18*, 259–341.
- (2) Nicole, L.; Laberty-Robert, C.; Rozes, L.; Sanchez, C. Hybrid materials science: a promised land for the integrative design of multifunctional materials. *Nanoscale* **2014**, *6*, 6267–6292.
- (3) Sanchez, C.; Julián, B.; Belleville, P.; Popall, M. Applications of hybrid organic–inorganic nanocomposites. *J. Mater. Chem.* **2005**, *15*, 3559–3592.
- (4) Schmidt, H. New type of non-crystalline solids between inorganic and organic materials. *J. Non-Cryst. Solids* **1985**, *73*, 681–691.
- (5) Rao, C. N. R.; Cheetham, A. K.; Thirumurugan, A. Hybrid inorganic–organic materials: a new family in condensed matter physics. *J. Phys. Condens. Matter.* **2008**, *20*, No. 083202.
- (6) Chujo, Y. Organic-inorganic hybrid materials. *Curr. Opin. Solid State Mater. Sci.* **1996**, *1*, 806–811.
- (7) Nguyen, V.; Perrin, F. X.; Vernet, J. L. Protective organic-inorganic hybrid coatings on mild steel derived from $\text{Ti}(\text{OC}_4\text{H}_9)_4$ -modified precursors. *Mater. Corros.* **2004**, *55*, 659–664.
- (8) Roux, S.; Audebert, P.; Pagetti, J.; Roche, M. Design of a new bilayer polypyrrole-xerogel hybrid coating for corrosion protection. *J. Mater. Chem.* **2001**, *11*, 3360–3366.
- (9) Voevodin, N. N.; Grebasch, N. T.; Soto, W. S.; Arnold, F. E.; Donely, M. S. Potentiodynamic evaluation of sol–gel coatings with inorganic inhibitors. *Surf. Coat. Technol.* **2001**, *140*, 24–28.
- (10) Langer, R. Selected advances in drug delivery and tissue engineering. *J. Controlled Release* **1999**, *62*, 7–11.
- (11) Kokubo, T.; Kushitani, H.; Sakka, S.; Kitsugi, T.; Yamamuro, T. Solutions able to reproduce in vivo surface-structure changes in bioactive glass-ceramic A-W. *J. Biomed. Mater. Res.* **1990**, *24*, 721–734.
- (12) Shi, J.; Jiang, Y.; Wang, X.; Wu, H.; Yang, D.; Pan, F.; Su, Y.; Jiang, Z. Design and synthesis of organic–inorganic hybrid capsules for biotechnological applications. *Chem. Soc. Rev.* **2014**, *43*, 5192–5210.
- (13) Díaz, U.; Brunel, D.; Corma, A. Catalysis using multifunctional organosiliceous hybrid materials. *Chem. Soc. Rev.* **2013**, *42*, 4083–4097.
- (14) Jiang, Y.; Gao, Q. Heterogeneous Hydrogenation Catalyses over Recyclable Pd(0) Nanoparticle Catalysts Stabilized by PAMAM-SBA-15 Organic–Inorganic Hybrid Composites. *J. Am. Chem. Soc.* **2006**, *128*, 1716–1717.
- (15) Wight, A. P.; Davis, M. E. Design and Preparation of Organic–Inorganic Hybrid Catalysts. *Chem. Rev.* **2002**, *102*, 3589–3614.
- (16) Millini, R.; Bellussi, G. Hybrid organic–inorganic zeolites: status and perspectives. *Catal. Sci. Technol.* **2016**, *6*, 2502–2527.
- (17) Zhang, X.; Jing, L.; Wei, L.; Zhang, F.; Yang, H. Semipermeable Organic–Inorganic Hybrid Microreactors for Highly Efficient and Size-Selective Asymmetric Catalysis. *ACS Catal.* **2017**, *7*, 6711–6718.
- (18) Zhou, D.; Xu, J.; Deng, J.; Wei, X.; Lu, X.; Chu, X.; Deng, F.; Xia, Q. One-step DGC assembly and structural characterization of a hairy particle zeolite-like organic–inorganic hybrid as an efficient modifiable catalytic material. *Dalton Trans.* **2015**, *44*, 14732–14740.
- (19) Li, L.; Niu, R.; Zhang, Y. Ag–Au bimetallic nanocomposites stabilized with organic–inorganic hybrid microgels: synthesis and their regulated optical and catalytic properties. *RSC Adv.* **2018**, *8*, 12428–12438.
- (20) Xu, L.; Li, C.-g.; Zhang, K.; Wu, P. Bifunctional tandem catalysis on multilamellar organic–inorganic hybrid zeolites. *ACS Catal.* **2014**, *4*, 2959–2968.
- (21) Dekamin, M. G.; Azimoshan, M.; Ramezani, L. Chitosan: a highly efficient renewable and recoverable bio-polymer catalyst for the expeditious synthesis of α -amino nitriles and imines under mild conditions. *Green Chem.* **2013**, *15*, 811–820.
- (22) Xu, X.; Liu, P.; Li, S.-h.; Zhang, P.; Wang, X.-y. Chitosan-supported imine palladacycle complex and its catalytic performance for Heck reaction. *React. Kinet. Catal. Lett.* **2006**, *88*, 217–223.
- (23) Saha, S.; Pal, A.; Kundu, S.; Basu, S.; Pal, T. Photochemical Green Synthesis of Calcium-Alginate-Stabilized Ag and Au Nanoparticles and Their Catalytic Application to 4-Nitrophenol Reduction. *Langmuir* **2010**, *26*, 2885–2893.
- (24) Gates, B. C.; Knozinger, H. Physical characterization of solid catalysts in the functioning state. *Adv. Catal.* **2006**, *49*, 1–382.
- (25) List, B. Emil Knoevenagel and the Roots of Aminocatalysis. *Angew. Chem., Int. Ed.* **2010**, *49*, 1730–1734.
- (26) Soleimani, E.; Khodaei, M. M.; Batooei, N.; Baghbazadeh, M. Water-prompted synthesis of alkyl nitrile derivatives via Knoevenagel condensation and Michael addition reaction. *Green Chem.* **2011**, *13*, 566–569.
- (27) Fringuelli, F.; Piermatti, O.; Pizzo, F. One-Pot Synthesis of 3-Carboxycoumarins via Consecutive Knoevenagel and Pinner Reactions in Water. *Synthesis* **2003**, *15*, 2331–2334.
- (28) Narsaiah, A. V.; Nagaiah, K. An Efficient Knoevenagel Condensation Catalyzed by $\text{LaCl}_3 \cdot 7\text{H}_2\text{O}$ in Heterogeneous Medium. *Synth. Commun.* **2003**, *21*, 3825–3832.
- (29) Ramachary, D. B.; Chowdari, N. S.; Barbas, C. F. Organocatalytic Asymmetric Domino Knoevenagel/Diels-Alder Reactions: A Bioorganic Approach to the Diastereoselective and Enantioselective Construction of Highly Substituted Spiro[5,5]undecane-1,5,9-triones. *Am. Ethnol.* **2003**, *42*, 4233–4237.
- (30) Texier-Boullet, F.; Foucaud, A. Knoevenagel condensation catalysed by aluminium oxide. *Tetrahedron Lett.* **1982**, *23*, 4927–4928.
- (31) Yamawaki, J.; Kawate, T.; Ando, T.; Hanafusa, T. Potassium Fluoride on Alumina. An Efficient Solid Base for Elimination, Addition, and Condensation. *Bull. Chem. Soc. Jpn.* **1983**, *56*, 1885–1886.
- (32) Macquarrie, D. J.; Jackson, D. B. Aminopropylated MCMs as base catalysts: a comparison with aminopropylated silica. *Chem. Commun.* **1997**, *29*, 1781–1782.
- (33) Reddy, T. I.; Varma, R. S. Rare-earth (RE) exchanged NaY zeolite promoted Knoevenagel condensation. *Tetrahedron Lett.* **1997**, *38*, 1721–1724.
- (34) Choudary, B. M.; Lakshmi Kantam, M.; Neeraja, V.; Koteswara Rao, K.; Figueras, F.; Delmotte, L. Layered double hydroxide fluoride: a novel solid base catalyst for C–C bond formation. *Green Chem.* **2001**, *3*, 257–260.
- (35) Fihri, A.; Len, C.; Varma, R. S.; Solhy, A. Hydroxyapatite: A review of syntheses, structure and applications in heterogeneous catalysis. *Coord. Chem. Rev.* **2017**, *347*, 48–76.
- (36) Li, G.; Xiao, J.; Zhang, W. Efficient and reusable amine-functionalized polyacrylonitrile fiber catalysts for Knoevenagel condensation in water. *Green Chem.* **2012**, *14*, 2234–2242.
- (37) Luan, Y.; Qi, Y.; Gao, H.; Andriamantsoa, R. S.; Zheng, N.; Wang, G. A general post-synthetic modification approach of amino-tagged metal-organic frameworks to access efficient catalysts for the Knoevenagel condensation reaction. *J. Mater. Chem. A* **2015**, *3*, 17320–17331.
- (38) Sharma, P.; Sasson, Y. Highly active $\text{g-C}_3\text{N}_4$ as a solid base catalyst for Knoevenagel condensation reaction under phase transfer conditions. *RSC Adv.* **2017**, *7*, 25589–25596.
- (39) Butler, R. N.; Coyne, A. G. Water: Nature's Reaction Enforcer—Comparative Effects for Organic Synthesis “In-Water” and “On-Water.”. *Chem. Rev.* **2010**, *110*, 6302–6337.
- (40) Simon, M.-O.; Li, C.-J. Green chemistry oriented organic synthesis in water. *Chem. Soc. Rev.* **2012**, *41*, 1415–1427.
- (41) Breslow, R. The Principles of and Reason for Using Water as a Solvent for Green Chemistry. *Handb. Green Chem.* **2010**, *5*, 1–29.
- (42) Rideout, D. C.; Breslow, R. Hydrophobic acceleration of Diels-Alder reactions. *J. Am. Chem. Soc.* **1980**, *102*, 7816–7817.
- (43) Breslow, R. Structure and reactivity in aqueous solution. *ACS Symp. Ser.* **1994**, *568*, 291.
- (44) Breslow, R. A Fifty-Year Perspective on Chemistry in Water. *Organic reactions in water*, Ed. Lindstrom, M., Blackwell Oxford. 2007, 1–28.

- (45) Scherrmann, M. C.; Norsikian, S.; Lubineau, A. Solvophobic Activation in Organic Synthesis. *Adv. Org. Synth.* **2005**, *1*, 341–401.
- (46) Narayan, S.; Muldoon, J.; Finn, M. G.; Fokin, V. V.; Kolb, H. C.; Sharpless, K. B. "On Water:" Unique Reactivity of Organic Compounds in Aqueous Suspension. *Angew. Chem., Int.* **2005**, *44*, 3275–3279.
- (47) Jung, Y.; Marcus, R. A. On the Theory of Organic Catalysis "on Water." *J. Am. Chem. Soc.* **2007**, *129*, 5492–5502.
- (48) Chanda, A.; Fokin, V. V. Organic Synthesis "On Water." *Chem. Rev.* **2009**, *109*, 725–748.
- (49) Hayashi, Y. In Water or in the Presence of Water? *Angew. Chem., Int. Ed.* **2006**, *45*, 8103–8104.
- (50) Scherrmann, M. C.; Lubineau, A.; Queneau, Y. Functionalization of Carbohydrates in Water. *Handb. Green Chem.* **2010**, *5*, 291–330.
- (51) Scherrmann, M. C. Knoevenagel Reaction of Unprotected Sugars. *Top. Curr. Chem.* **2010**, *295*, 1–18.
- (52) Rodrigues, F.; Canac, Y.; Lubineau, A. A convenient, one-step, synthesis of β -C-glycosidic ketones in aqueous media. *Chem. Commun.* **2000**, 2049–2050.
- (53) Hersant, Y.; Abou-Jneid, R.; Canac, Y.; Lubineau, A.; Philippe, M.; Semeria, D.; Radisson, X.; Scherrmann, M.-C. One-step synthesis of β -C-glycolipid derivatives from unprotected sugars. *Carbohydr. Res.* **2004**, *339*, 741–745.
- (54) Bragnier, N.; Scherrmann, M.-C. One-step synthesis of β -C-glycosidic ketones in aqueous media: the case of 2-acetamido sugars. *Synthesis* **2005**, *2005*, 814–818.
- (55) Leseurre, L.; Genêt, J.-P.; Michelet, V. Coupling reactions in water. *Handb. Green Chem.* **2010**, *5*, 151–206.
- (56) Bozzel, J. B. Green chemistry in practice. *Handbook of Green Chemistry and Technology* (Eds: Clark, J.; Macquarrie, D.), Chapter 14, Blackwell: Oxford. 2002, DOI: 10.1002/9780470988305.ch14.
- (57) Joó, F.; Kathó, A. Water as a Green Solvent for Bulk Chemicals. *Handb. Green Chem.* **2010**, *5*, 385–408.
- (58) Cornils, B. Industrial aqueous biphasic catalysis: status and directions. *Org. Proc. Res. Dev.* **1998**, *2*, 121–127.
- (59) Amer, W.; Abdelouahdi, K.; Ramanarivo, H. R.; Fihri, A.; El Achaby, M.; Zahouily, M.; Barakat, A.; Djessas, K.; Clark, J.; Solhy, A. Smart designing of new hybrid materials based on brushite-alginate and monetite-alginate microspheres: Bio-inspired for sequential nucleation and growth. *Mater. Sci. Eng. C.* **2014**, *35*, 341–346.
- (60) Ramanarivo, H. R.; Maati, H.; Amadine, O.; Abdelouahdi, K.; Barakat, A.; Ihiwakrim, D.; Ersen, O.; Varma, R. S.; Solhy, A. Ecofriendly synthesis of ceria foam via carboxymethylcellulose gelation: application for the epoxidation of chalcone. *ACS Sustainable Chem. Eng.* **2015**, *3*, 2786–2795.
- (61) Ramanarivo, H. R.; Abdelouahdi, K.; Amer, W.; Zahouily, M.; Clark, J.; Solhy, A. Tunable structure of zirconia nanoparticles by biopolymer gelation: design, synthesis and characterization. *Eur. J. Inorg. Chem.* **2012**, 5465–5469.
- (62) Ribeiro, C. C.; Barrias, C. C.; Barbosa, M. A. Calcium phosphate-alginate microspheres as enzyme delivery matrices. *Biomaterials* **2004**, *25*, 4363–4373.
- (63) Teng, S.; Shi, J.; Peng, B.; Chen, L. The effect of alginate addition on the structure and morphology of hydroxyapatite/gelatin nanocomposites. *Compos. Sci. Technol.* **2006**, *66*, 1532–1538.
- (64) Stulajterova, R.; Medvecký, L. Effect of calcium ions on transformation brushite to hydroxyapatite in aqueous solutions. *Colloids Surf., A* **2008**, *316*, 104–109.
- (65) Shkilnyy, A.; Brandt, J.; Manton, A.; Paris, O.; Schlaad, H.; Taubert, A. Calcium phosphate with a channel-like morphology by polymer templating. *Chem. Mater.* **2009**, *21*, 1572–1578.
- (66) Mandel, S.; Tas, A. C. Brushite ($\text{CaHPO}_4 \cdot 2\text{H}_2\text{O}$) to octacalcium phosphate ($\text{Ca}_8(\text{HPO}_4)_2(\text{PO}_4)_4 \cdot 5\text{H}_2\text{O}$) transformation in DMEM solutions at 36.5 °C. *Mater. Sci. Eng. C.* **2010**, *30*, 245–254.
- (67) Toshima, T.; Hamai, R.; Tafu, M.; Takemura, Y.; Fujita, S.; Chohji, T.; Tanda, S.; Li, S.; Qin, G. W. Morphology control of brushite prepared by aqueous solution synthesis. *J. As. Ceram. Soc.* **2002**, *2*, 52–56.
- (68) Stephan, D. W. Frustrated Lewis Pairs. *J. Am. Chem. Soc.* **2015**, *137*, 10018–10032.